

Electrochemical screening of self-assembling β -sheet peptides using supported phospholipid monolayers

E. Protopapa^a, A. Aggeli^a, N. Boden^a, P.F. Knowles^b, L.C. Salay^{a,1}, A. Nelson^{a,*}

^a Center for Self Organising Molecular Systems, School of Chemistry, University of Leeds, LS2 9JT, UK

^b School of Biochemistry and Molecular Biology, University of Leeds, LS2 9JT, UK

Received 28 April 2006; accepted 4 May 2006

Abstract

In the context of the medical applications of β -sheet self-assembling peptides, it is important to be able to predict their activity at the biological membrane level. A study of the interaction of four systematically varied 11-residue (P11-1, P11-2, P11-6 and P11-7) and one 13-residue (P13-1) designed β -sheet self-assembling peptides with DOPC monolayers on a mercury electrode is reported in this paper. Experiments were carried out in 0.1 mol dm⁻³ KCl electrolyte with added phosphate buffer (0.001 mol dm⁻³) at pH \sim 7.6. The capacity–potential curves of the coated electrode in the presence and absence of the different peptides were measured using out-of-phase ac voltammetry. The frequency dependence of the complex impedance of the coated electrode surfaces in the presence and absence of the peptides was estimated between 65,000 and 0.1 Hz at -0.4 V versus Ag/AgCl 3.5 mol⁻³ dm⁻³ KCl. The monolayer permeabilising properties of the peptides were studied by following the reduction of Tl(I) to Tl(Hg) at the coated electrode. Of the five peptides studied, P11-2, P11-7 and P13-1 interact most strongly with the DOPC layer. P11-1 which has a polar primary structure shows no obvious interaction with the phospholipid but surprisingly, it permeabilises the phospholipid layer to Tl⁺.

© 2006 IPPEM. Published by Elsevier Ltd. All rights reserved.

Keywords: Phospholipid monolayers; Self-assembling beta-sheet peptides; Capacitance; Tl(I) permeability; Tryptophan; Screening

1. Introduction

The interaction of biologically active peptides with biological membranes in particular the phospholipid component has received much interest in the last decade [1–12]. The results have relevance to biological mechanisms since peptide and protein interactions with biological membranes are of great significance in many aspects of physiology [7], such as cell signalling and toxicology. Of particular interest are the antimicrobial peptides [1,2,5,6,9–12] and the membrane-active peptides [3], which act by disrupting biological membrane structure and function. The ability of antimicrobial peptides to kill bacteria while not disrupting native cells is

attracting a great deal of attention, especially since traditional antibiotics are becoming increasingly difficult to produce and because of increased bacterial mutation. The mechanism of action of antimicrobial peptides is not entirely understood, but it is clear that they interact not with membrane proteins, but with the lipid matrix itself, and therefore leave little or no possibility for mutation which could affect their performance.

Three models of membrane rupturing mechanisms have been proposed to date: barrel-stave [13–17], carpet [18,19], and toroidal [20–22]. According to the barrel-stave model, peptides bound to the membrane recognize each other and oligomerize. Upon oligomerization, antimicrobial peptides orient themselves, allowing the hydrophobic surface to interact with the hydrophobic core of the membrane and the hydrophilic surface to point inward to create a hydrophilic transmembrane pore. The carpet model suggests that antimicrobial peptides initially bind to and cover the surface of the target membrane. The electrostatic interaction between the peptide and the lipid head group imposes strain in the

* Corresponding author. Tel.: +44 113 6409; fax: +44 113 6452.

E-mail address: andrewn@chem.leeds.ac.uk (A. Nelson).

¹ Present address: Laboratory of Structural Biology, Department of Biochemistry, Institute of Chemistry, University of Sao Paulo, CP 26077, 05513-970 Sao Paulo, Brazil.

membrane, and membrane permeation is induced only at sites where local peptide concentration is higher than certain threshold values. In the toroidal model, peptides similarly bind and interact with lipid head groups, imposing a positive curvature strain on the membrane (e.g., magainin 2) and producing channels where the polar headgroup region expands to form “toroidal” pores. In these mechanisms, the interaction between the phospholipid component of the membrane and the peptide is often of particular importance [23,24]. Because of this phospholipid–peptide interactions are the subject of considerable interest.

Several molecular properties of the peptides are known to promote interaction with the phospholipid such as hydrophobicity [25], number of residues [26] and the presence of specific peptide residues such as tryptophan [26].

In order to study the interaction of peptides with biological membranes, biological membrane models are often used [27]. These represent a significant approach since the experimental conditions can be rigorously controlled and selective aspects of the interaction can be investigated. Membrane models used to study phospholipid–peptide interaction have ranged from free-standing bilayers [27] to monolayers at the air–water [28] interface to supported monolayers and bilayers [29]. One of the most powerful supported membrane models available is that of a phospholipid monolayer/bilayer on a mercury electrode [30]. The great advantage is its inherent reproducibility and ease of use and the ability to control the potential and measure the current very precisely. The system has acted as a good host for the gramicidin monomolecular channel so that channel function can be monitored using the $Tl^+/Tl(Hg)$ system as a redox probe [31]. At the same time interactions with the phospholipid monolayer can be investigated since the pure monolayer system is virtually defect-free and self-sealing. Any modification to the structure can be easily monitored. Electrochemical methods of impedance are a very sensitive way to monitor the structure and properties of the layer and a novel impedance model has been developed using the system to test it [32]. Recently an investigation of the interaction of gramicidin peptide derivatives with the monolayer was carried out using voltammetric and impedance techniques [33]. Results were encouraging and they correlated well with those of independent experiments carried out with membrane models of monolayers at the air–water interface. This has provided the instigation to use the system to study interactions with other peptides. In order to isolate the molecular principles associated with the interaction it was deemed appropriate to use custom designed peptides. In this case the type of phospholipid–peptide interaction could be related to specific molecular characteristics.

This paper reports on the interaction of custom designed peptides with phospholipid monolayers of dioleoyl phosphatidylcholine (DOPC) on mercury. The particular techniques used were: (i) ac voltammetry to examine the effect of peptide interaction on the phospholipid phase transitions in capacitance–potential curves, (ii) ac impedance to look at the extent of penetration of peptide into the monolayer

and any modifying effect on the monolayer structure from impedance–frequency data, and (iii) sampled-current voltammetry of the $Tl^+/Tl(Hg)$ redox probe to look for permeabilising effects of the peptide.

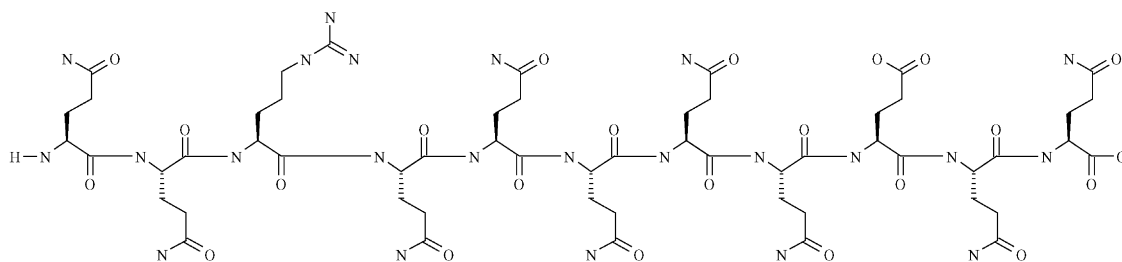
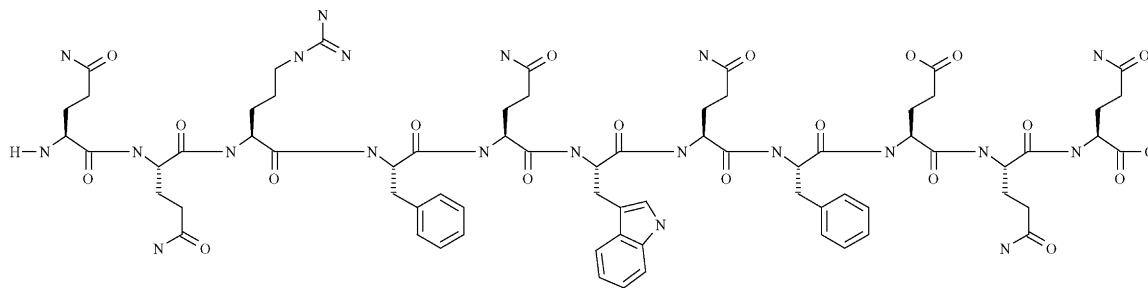
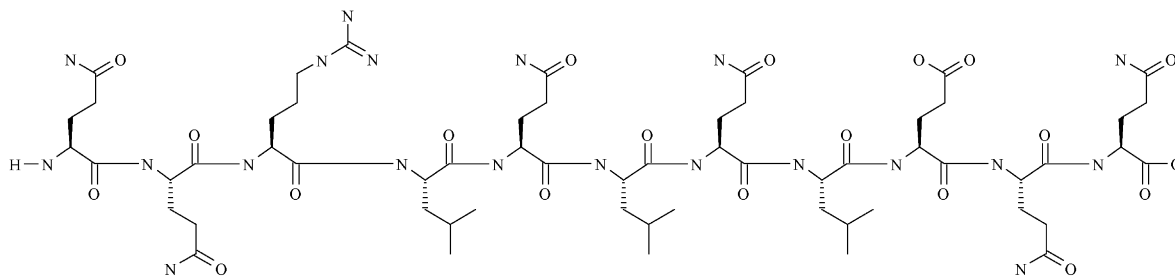
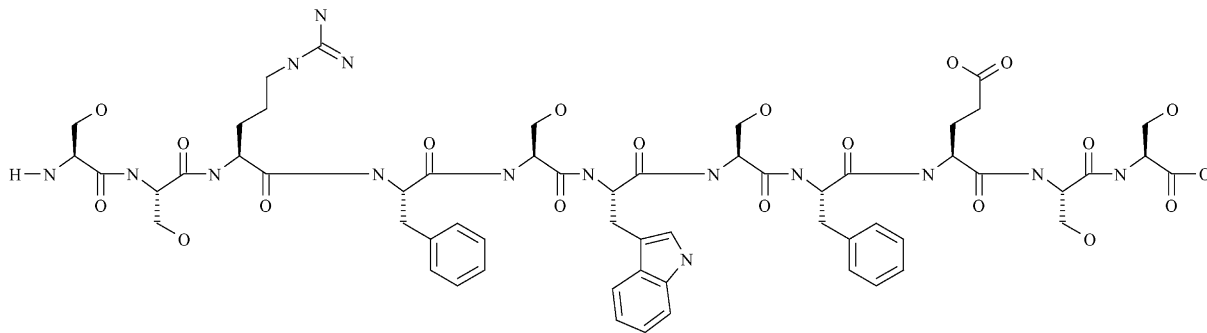
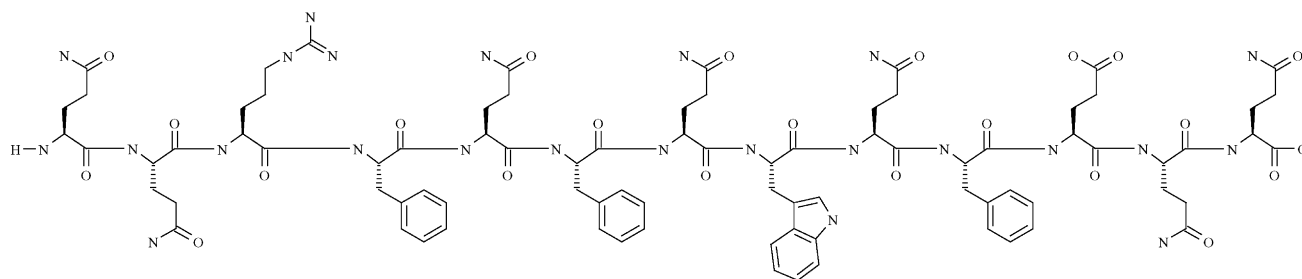
In recent years, the biological β -sheet motif has been exploited to design simple *de novo* peptides that self-assemble in a hierarchical manner to form a variety of well-defined twisted elongated nanostructures [34–37] such as tapes (single molecule in thickness), ribbons (a pair of stacked tapes back to back), fibrils (a bundle of stacked ribbons) and fibres (a pair of fibrils interacting edge-to-edge). A theoretical model has been developed to rationalise this self-assembly process [38,39]. At concentrations typically higher than 0.5% (v/v) in solution these micrometer-long aggregates can form isotropic solid-like organogels and hydrogels, as well as nematic liquid crystalline fluids and gels. The self-assembly can be switched on or off by a variety of external chemical triggers such as pH and ionic strength [40,41]. On the one hand these peptides provide an ideal model system for the investigation of the principles that drive biomolecular peptide self-assembly, and in particular the formation and stabilisation of elongated β -sheet structures, e.g. present in amyloid diseases. On the other hand the mechanical, structural and bioactive properties as well as the surface chemistry of these systems can be finely controlled by appropriate peptide design. Therefore, there is the opportunity to design self-assembling peptides with a combination of properties appropriate for specific applications, e.g. in the biomedical field such as scaffolds for tissue engineering, or biomaterials for personal care and dental hygiene. In the light of these applications, it was considered appropriate to test the putative membrane-activity of these β -self-assembling peptides using the DOPC coated electrode system.

The structures of the peptides tested in this study are shown in Scheme 1.

2. Experimental

2.1. Apparatus and materials

Two distinct measurements were carried out using the electrochemical apparatus. The first series of measurements focused on impedance measurements in which no faradaic process is involved. These experiments concentrated on capacitive elements [30,32,33]. The second series investigated the transport of Tl^+ ions in which a faradaic process is involved [31]. The rationale for using Tl^+ as a probe is the following. (1) Tl^+ is isoelectronic with K^+ and thus it is an effective probe for this ion's behaviour and the alkali metal ions in general. (2) Tl^+ undergoes a rapid reversible redox reaction on the mercury surface with a reduction potential at about -0.42 V versus $Ag/AgCl$, 3.5 mol dm^{-3} KCl which is in the potential domain of the low capacity and ion impermeable region of the DOPC monolayer. As a consequence

P11-1³⁷P11-2³⁷P11-6⁴²P11-7^{43,44}P13-1⁴²

Scheme 1.

in the presence of the DOPC monolayer the electrochemical reduction of Tl^+ is suppressed because Tl^+ is denied access to the mercury surface. When the DOPC monolayer is permeabilised a reduction current of Tl^+ is observed. The results of both impedance and voltammetric measurements are considered in terms of the properties of the phospholipid and modified phospholipid monolayer.

A home made potentiostat connected to a function generator and lock-in-amplifier interfaced to a MacLab acquisition board and software was used to measure capacitance–potential curves of the coated electrodes. An Autolab system, FRA and PGSTAT 30 interface (Ecochemie, Utrecht, The Netherlands), controlled with Autolab software, was used in all the impedance versus frequency measurements of the coated electrodes. A home made potentiostat connected to a MacLab acquisition board and software (AD Instruments Ltd.) was used in the sampled-current voltammetry experiments to measure the reduction of Tl^+ . The experiments were performed in a standard three electrode cell. An Ag/AgCl, 3.5 mol dm^{-3} KCl reference electrode with a porous sintered glass frit separating the 3.5 mol dm^{-3} KCl solution from the electrolyte served as reference and a platinum bar served as counter electrodes located on either side of the working electrode, respectively. In the impedance–frequency measurements, a solution resistance of around $280\text{--}300 \Omega$ was recorded for the cell [32,33]. Diagnostic plots of the impedance data showed it to be that of an RC series circuit as before [32,33]. There was a distinct absence of instability at high frequencies and for this reason, the use of a fourth pseudo-reference electrode was not considered necessary at this stage.

The electrolyte, KCl (0.1 mol dm^{-3}) was prepared from Analar KCl (Fisher Chemicals Ltd.) calcined at 600°C and dissolved in $18.2 \text{ M}\Omega$ MilliQ water with added $0.001 \text{ mol dm}^{-3}$ phosphate buffer. A blanket of argon gas was maintained above the fully deaerated electrolyte during all experiments. Monolayers of DOPC were prepared as described earlier [30–33] by initially spreading $13 \mu\text{m}^3$ of a 2 mg cm^{-3} solution of DOPC in pentane (HPLC grade, Fisher Scientific Chemicals Ltd.) at the argon–electrolyte interface in the electrochemical cell [30–33]. The working solution of DOPC was obtained by dilution of the 20 mg cm^{-3} stock solution (Lipid Products, UK). A fresh mercury drop (area, $A = 0.0092 \text{ cm}^2$) was coated with the spread phospholipid [30–33] layer at the argon–electrolyte interface prior to each series of experiments to give a monolayer coated electrode.

Aliquots of the respective working solutions of peptide were injected below the layer into the electrolyte. The solution was then gently stirred for 5 min. The phospholipid monolayer was then deposited on the electrode. Such layers in this study are referred to as peptide modified layers regardless of the extent of interaction. In the experiments studying the $Tl(I)/Tl(Hg)$ reduction, $TlNO_3$ (Sigma Products) was employed to prepare the stock solution (0.1 mol dm^{-3}) from which aliquots were added to the electrolyte.

2.2. Electrochemical impedance

Measurements of capacity versus potential for the coated electrode were carried out by measuring the out-of-phase current (I'') at potentials between -0.2 and -1.2 V at a frequency (f) of 75 Hz with $0.0046 \text{ V}_{\text{rms}}$ (ΔV) using the ac voltammetric method. Capacitance (C_d) was calculated from the I'' value using the equation $C_d = (I''/A \Delta V \omega)$ where ω is the angular frequency ($=2\pi f$) assuming RC series behaviour of the cell [30].

The capacitance–potential curve of the DOPC coated electrode was recorded prior to each experiment. At least two capacitance–potential curves following respective depositions on a fresh electrode surface were recorded for the individual peptide–phospholipid interactions.

Measurements of the impedance (Z) versus frequency of the electrode systems using frequencies logarithmically distributed from $65,000$ to 0.1 Hz , $0.005 \text{ V}_{\text{rms}}$ at potentials of -0.4 V were carried out on the coated electrode systems. The impedance versus frequency plot of the DOPC coated electrode was recorded prior to each experiment. At least three impedance versus frequency plots following respective depositions on the fresh electrode surface were recorded for the individual peptide–phospholipid interactions. The experimental conditions for the measurement of impedance are listed in the following. For one measurement, one cycle was used except when the cycle was less than 1 s, in which case, the measurement time was 1 s. In order to reach steady state, 10 cycles were used except when 10 cycles lasted more than 3 s, in which case, 3 s were used. Each frequency scan took 5 min with the potential continually applied commencing with the highest frequency. These time intervals are a compromise in providing sufficient time to carry out the measurement and reaching steady state, whilst still enabling all the experiments to be done within a specified time period on one phospholipid layer without altering the structure of the layer. No significant difference in the spectra was noted when longer equilibration periods were used before each experiment. The impedance data were transformed to the complex capacitance plane and the complex capacitance axes were expressed as $\text{Re } Y\omega^{-1}$ and $\text{Im } Y\omega^{-1}$, respectively. This was done using the EXCEL (Microsoft) spreadsheet. Curve fitting of the data was carried out using IGOR (Wavemetrics) in the same way as described previously [32,33].

Due to the absence of any electroactive component, the simplest equivalent circuit model is the uncompensated solution resistance (R_u) of the cell and the capacitance (C) of the working electrode in series [45]. R_u can be determined by extrapolating the $\text{Im } Z$ versus $\text{Re } Z$ plot to the $\text{Re } Z$ axis [46]. In the complex capacitance plane, values of $\text{Re } Y\omega^{-1}$ were plotted against $\text{Im } Y\omega^{-1}$ for all values of frequency [46–48]. For a series RC circuit, the $\text{Re } Y\omega^{-1}$ versus $\text{Im } Y\omega^{-1}$ plots gives a single semi-circle for the RC element, where the capacitor has no frequency dispersion. The extrapolation of this semi-circle to the $\text{Im } Y\omega^{-1}$ axis at low frequency gives the zero frequency capacitance (ZFC equivalent to C) [46–48] of the RC circuit which is therefore an empirical quantity. When

applied to the phospholipid-coated electrode any additional elements to the RC semi-circle at lower frequencies will correspond to properties of the phospholipid layer. Further, if the semi-circle representing the RC element is not perfect [49], the non-ideality of the capacitor is indicated. This can be due to dielectric relaxations coupled to the RC charging process and to additional circuit elements at the interface between the capacitor and the solution resistance [50].

Representative impedance data were fitted to Eq. (1) below as done previously [31,32]:

$$Y = \frac{1}{R + \frac{1}{(i\omega)^\beta \omega_0^{1-\beta} \left[\frac{C_s - C_{\text{inf}}}{1 + (i\omega\tau)^\alpha} + C_{\text{inf}} \right]}} \quad (1)$$

In Eq. (1), Y is the admittance, R equivalent to the uncompensated solution resistance (R_u), C_{inf} equivalent to the zero frequency capacitance (ZFC) of the monolayer, $C_s - C_{\text{inf}}$ the additional low frequency capacitive element with relaxation time constant, (τ), α the coefficient which represents the distribution of time constants around a most probable value (the lower the α value below unity, the more diffuse the distribution) and β is the coefficient which characterises non-idealities at the interface between R and C and is equivalent to a “surface roughness” [49] (the lower the β value below unity, the more non-ideal or “rougher” the interface). $\omega_0^{1-\beta}$ is a dummy constant which corrects for units.

2.3. Electrochemistry of $\text{Ti}^+/\text{Ti}(\text{Hg})$

The following procedure [31] was taken to measure the peptide permeabilising activity to Ti^+ of the monolayer. Subsequent to deaeration of the electrolyte, $10^{-4} \text{ mol dm}^{-3}$ $\text{Ti}(\text{I})$ was added from the stock solution. The DOPC layer was then spread on the electrolyte and transferred to the electrode. A cyclic voltammogram was recorded to check the impermeability of the deposited layer. Following addition of peptide to the electrolyte and stirring, the phospholipid layer was deposited on the electrode surface. A series of voltage pulses from -0.2 V to potentials from -0.3 to -0.7 V and back were initiated and the current transients recorded. The pulses were 40 ms long and the currents were sampled at 40 kHz with a 20 kHz low pass filter. A delay period of 15 s between each pulse enabled the establishment of initial concentration conditions. After the pulsing programme had been performed, an ac out-of-phase voltammogram was recorded to ensure that the phospholipid layer had not degraded during the experiment. Pulse transients were analysed by sampling the current transient after a time interval of 2.5 ms from the beginning of the pulse and plotting this current value against potential as a sampled-current voltammogram. The currents were measured for the cathodic train of pulses and the anodic train of pulses. The mean current value and the range between the two values expressed as an error bar were recorded at each potential.

The entire current transient was fitted to the model describing a homogeneous chemical reaction preceding a rapid elec-

tron transfer ($C_r E_r$ mechanism). The equation characterising this model is written as [51]:

$$i(t) = \frac{FAD^{1/2}c_0}{1 - K^2} \times \left[\frac{K(e^{-kt} - K)}{\pi^{1/2}t^{1/2}} + e^{Bt} \{ [K(k + B)^{1/2} \times \text{erf}[(k + B)^{1/2}t^{1/2}] - B^{1/2}\text{erf}(B^{1/2}t^{1/2})] \} \right] \quad (2)$$

In Eq. (2), $k = k_1 + k_{-1}$ and k_1 and k_{-1} are the forward and reverse homogeneous rate constants, respectively of the chemical step of which $K (= k_1/k_{-1})$ is the equilibrium constant. k represents the rate of attainment of chemical equilibrium prior to the charge transfer. $B = K^2k/(1 - K^2)$. The important feature of Eq. (2) is that it is valid for all values of K provided $k_{-1} > k_1$ and for current data obtained over all real time. This equation simplifies to the following equation at longer time scales where $k_1^{\text{het}} = Kk^{1/2}D^{1/2}$ [52] and k_1^{het} is a heterogeneous rate constant describing the intrinsic monolayer permeability to Ti^+ at a specified potential:

$$i = FAc_0k_1^{\text{het}} \exp \left(\left(\frac{(k_1^{\text{het}})^2}{D} \right) t \right) \text{erfc} \left(\left(\frac{k_1^{\text{het}}}{D^{1/2}} \right) t^{1/2} \right) \quad (3)$$

Expressed in this way, Eq. (3) is referred to as the approximate equation describing the potential step current transient resulting from the $C_r E_r$ mechanism [53]. When Eq. (2) is fitted to the current transients, the time constant of the initial exponential decay corresponds to k^{-1} [31,52].

Curve fitting of the data was carried out using the IGOR programme as before [31].

2.4. Preparation of peptide solutions

Peptide production was carried out using standard solid phase *Fmoc* peptide synthesis protocol. The HPLC-purified peptides were checked by analytical HPLC, mass spectrometry and amino acid analysis. The mass spectra showed in each case only one main peak corresponding to the expected molecular weights: 1497.5 Da for P11-1, 1594 Da for P11-2, 1452.6 Da for P11-6, 1346.7 Da for P11-7 and 1896 Da for P13-1.

Peptides were dissolved in 3,3,3-trifluoroethanol (TFE) (Fisher Chemicals Ltd.) at 5 g dm^{-3} , vortexed and sonicated until a homogenous solution was obtained, and immediately distributed in aliquots to different vials and kept in the freezer. One vial was taken out of the freezer before the start of an experiment. The remainder of the solution in a vial was discarded at the end of the experiment.

3. Results

3.1. Effect of peptide interaction with DOPC on the impedance of the monolayer

Figs. 1 and 2 show the effect of the addition of peptide to the electrolyte on representative capacitance–potential

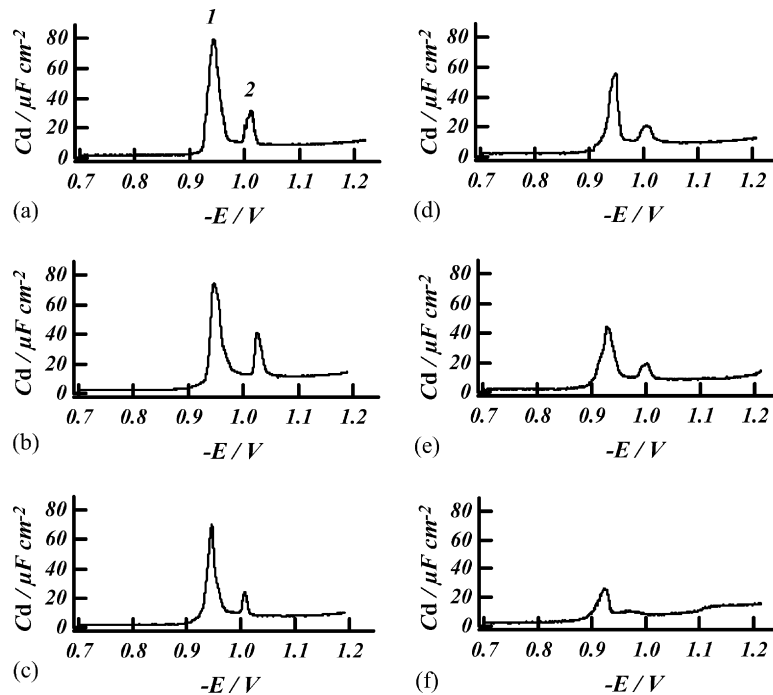


Fig. 1. Representative capacity–potential curves recorded on cathodic voltage sweep of DOPC coated electrodes in 0.1 mol dm^{-3} KCl with $0.001 \text{ mol dm}^{-3}$ phosphate buffer with (a) no added peptide (capacitance peaks 1 and 2 indicated) and (b)–(f) $1.2 \mu\text{mol dm}^{-3}$ of the following added peptides: (b) P11-1, (c) P11-6, (d) P11-7, (e) P13-1 and (f) P11-2.

curves (cathodic (Fig. 1) and anodic (Fig. 2) scans) of the DOPC monolayer. The effect of the peptides in solution ($1.12 \mu\text{mol dm}^{-3}$) in depressing capacitance peak 1 on the forward scan follows the order for increasing suppression: $\text{P11-1} < \text{P11-6} \ll \text{P11-7} \cong \text{P13-1} \cong \text{P11-2}$. This

effect is more significant on the reverse scans than the forward scans and the order of peptides in increasing peak suppression resulting from their presence in solution is: $\text{P11-6} < \text{P11-1} \ll \text{P11-2} \cong \text{P11-7} \cong \text{P13-1}$. This is also evident in Fig. 3 which shows the effect of the peptide

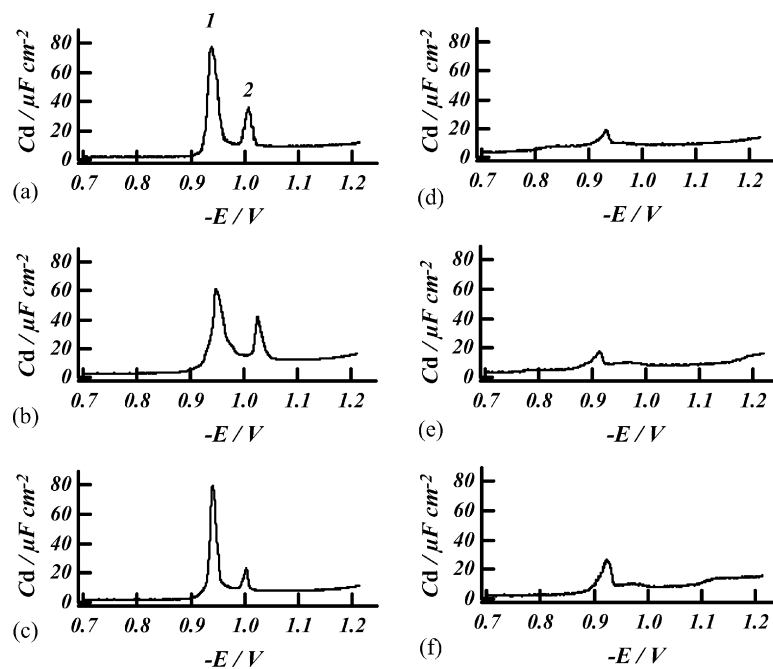


Fig. 2. Representative capacity–potential curves recorded on anodic voltage sweep of DOPC coated electrodes in 0.1 mol dm^{-3} KCl with $0.001 \text{ mol dm}^{-3}$ phosphate buffer and (a) no added peptide (capacitance peaks 1 and 2 indicated) and (b)–(f) $1.2 \mu\text{mol dm}^{-3}$ of the following added peptides: (b) P11-1, (c) P11-6, (d) P11-7, (e) P13-1 and (f) P11-2.

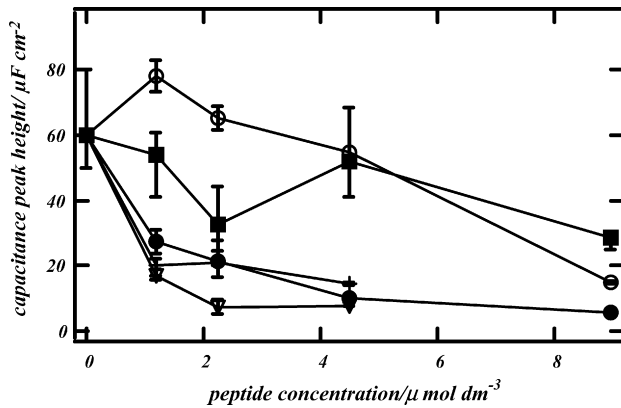


Fig. 3. Capacitance value of capacitance peak 1 from capacity–potential curves recorded on anodic voltage sweep of DOPC coated electrodes in 0.1 mol dm^{-3} KCl with $0.001 \text{ mol dm}^{-3}$ phosphate buffer and the following added peptides: P11-1 (filled square), P11-6 (open circle), P11-7 (open triangle), P13-1 (cross) and P11-2 (filled circle). Symbols express mean, and error bars express total range, of two or more measurements. Where no error bars are observed, they are within the symbol size.

interaction on capacitance peak 1 throughout the range of concentrations of the peptide in solution where the order of effect is more or less retained. The clearest difference in effect on the monolayer capacitance–potential curve

between the first group of peptides, P11-6 and P11-1 and the second group of peptides, P11-2, P11-7 and P13-1 is noted for the 1.2 nmol dm^{-3} peptide additions. The markers and error bars in Fig. 3 express means and range of values, respectively. In general two or more measurements were taken relating to each peptide–DOPC interaction. The peak height of the capacitance peak of the pure DOPC coated electrode was recorded from all the measurements.

Fig. 4 shows plots in the complex capacitance plane of transformed impedance data obtained from DOPC coated mercury in solutions with added peptides ($2.24 \mu\text{mol dm}^{-3}$). Control experiments without peptide added to the electrolyte were also carried out. The most accessible parameter is the zero frequency capacitance (ZFC) which can be measured directly from the complex capacitance plots. The order of peptide which causes the increase in ZFC of the monolayer in order of increasing effect is: $\text{P11-6} \cong \text{P11-1} < \text{P11-2} \cong \text{P13-1} < \text{P11-7}$. In addition it is only peptides P11-2, P13-1 and P11-7 which give rise to a significant second capacitive element outside of the RC semi-circle. The model of Whitehouse et al. [32,33] (Eq. (1)) was applied to the data from the interaction of P11-7 with DOPC which shows the most significant extra capacitive element. The fit is displayed in Fig. 4. Results for the coefficients together with their

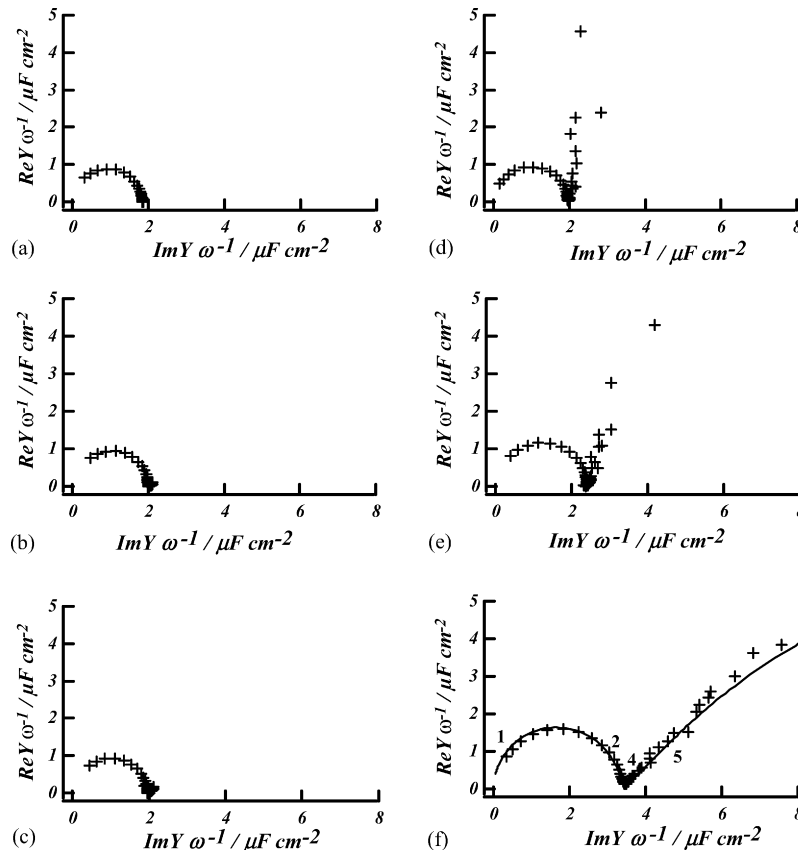


Fig. 4. Plots in complex capacitance plane of representative impedance data derived from DOPC in 0.1 mol dm^{-3} KCl with $0.001 \text{ mol dm}^{-3}$ phosphate buffer and (a) no added peptide and (b)–(f) $2.24 \mu\text{mol dm}^{-3}$ of the following added peptides: (b) P11-1, (c) P11-6, (d) P13-1, (e) P11-2 and (f) P11-7. Fit of Eq. (1) to data shown as solid line. Numbers on the plots indicate frequencies of adjacent data points expressed as and representing values in $\log(\omega \text{ (rad s}^{-1}\text{)})$ as follows: 1, 5.61; 2, 4.42; 4, 2.05; 5, 0.87.

Table 1

Values of coefficients \pm S.D. extracted from fit of Eq. (1) to impedance data derived from DOPC coated mercury electrode with peptide in electrolyte

Coefficient	2.24 $\mu\text{mol dm}^{-3}$ P11-7	0.13 $\mu\text{mol dm}^{-3}$ gramicidin A [33]
α	0.58 ± 0.02	1 ± 0.04
β	0.989 ± 0.003	0.981 ± 0.001
$C_s - C_{\text{inf}}$ ($\mu\text{F cm}^{-2}$)	23 ± 5	8.8 ± 5.2
τ (s)	13.01 ± 7.3	5.8 ± 4

errors are displayed in Table 1. These values are compared with those derived from the impedance data for DOPC in the presence of gramicidin derivatives [33]. The main difference is the decreased α value which is close to unity when extracted from the data of DOPC–gramicidin A interaction [33].

3.2. Effect of peptide interaction with DOPC on the $\text{Tl(I)}/\text{Tl(Hg)}$ redox process

Fig. 5 shows the sampled-current voltammograms of the Tl^+ reduction at the uncoated and coated mercury electrodes. The reduction of Tl^+ at the uncoated electrode appears as a reversible wave with a plateau height as predicted from the Cottrell equation with the given experimental conditions. A monolayer of DOPC on the electrode suppresses the reduction. P11-2 modified DOPC facilitates Tl^+ reduction and this is dependent to some extent on the P11-2 concentration in solution. P11-7 modified DOPC also facilitates Tl^+ reduction but the height of the reduction wave is not related to the peptide concentration in solution. P11-1 facilitates Tl^+ reduction to some extent but as with P11-7, there is no dependence of the height of the reduction

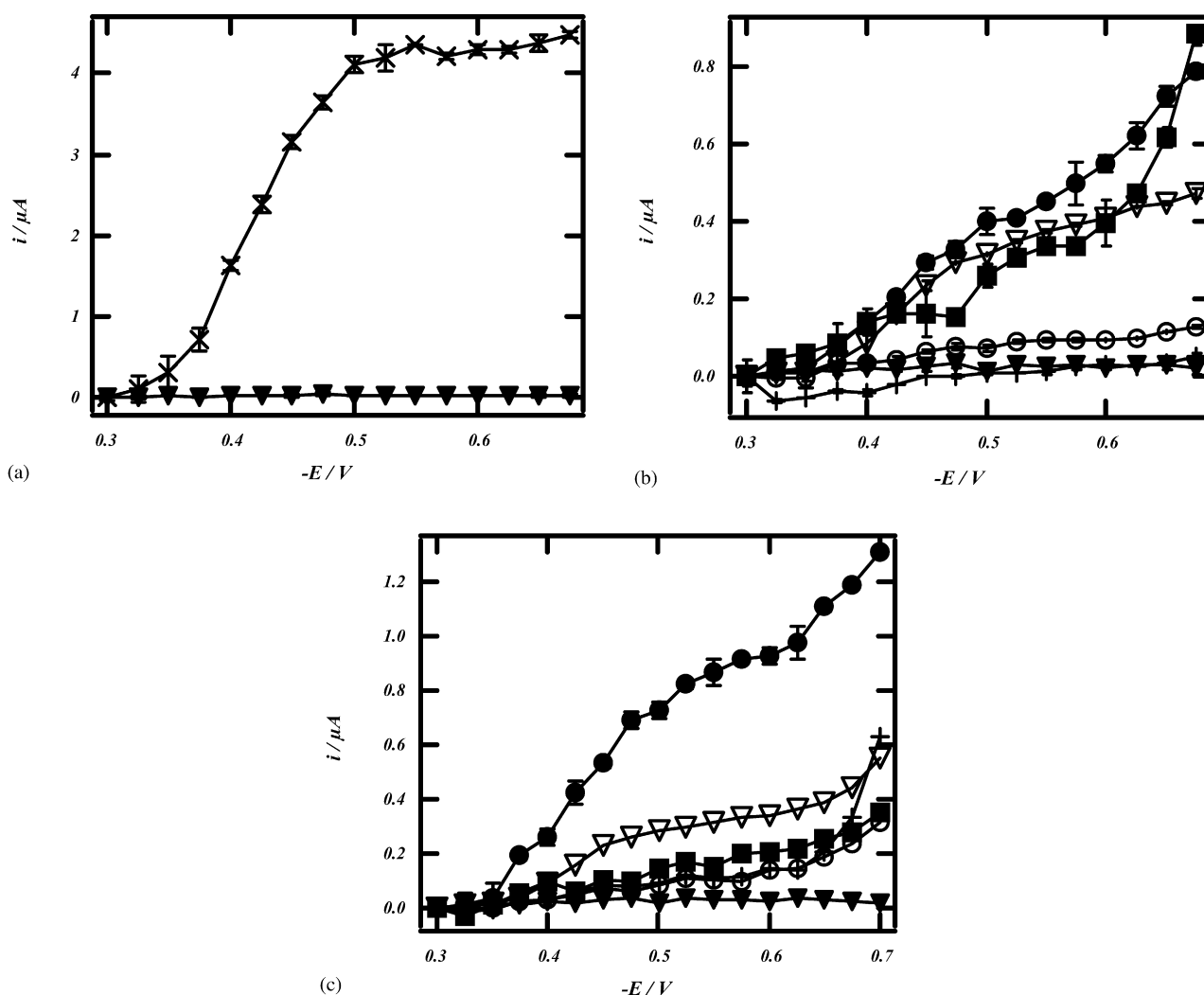


Fig. 5. Sampled-current voltammograms of the reduction of Tl^+ in 0.1 mol dm^{-3} KCl and $0.001 \text{ mol dm}^{-3}$ phosphate buffer with added Tl(I) ($10^{-4} \text{ mol dm}^{-3}$). (a) No peptide in electrolyte at DOPC coated (filled triangle) and uncoated (cross) mercury, (b) and (c) DOPC coated mercury with no peptide (filled triangle) and the following added peptides to electrolyte: P11-1 (filled square), P11-6 (open circle), P11-7 (open triangle), P13-1 (cross) and P11-2 (filled circle) at 2.24 (b) and 8.96 (c) $\mu\text{mol dm}^{-3}$. Symbols express mean, and error bars express total range, of current values from the cathodic and anodic train of pulses, respectively. Where no error bars are observed, they are within the symbol size.

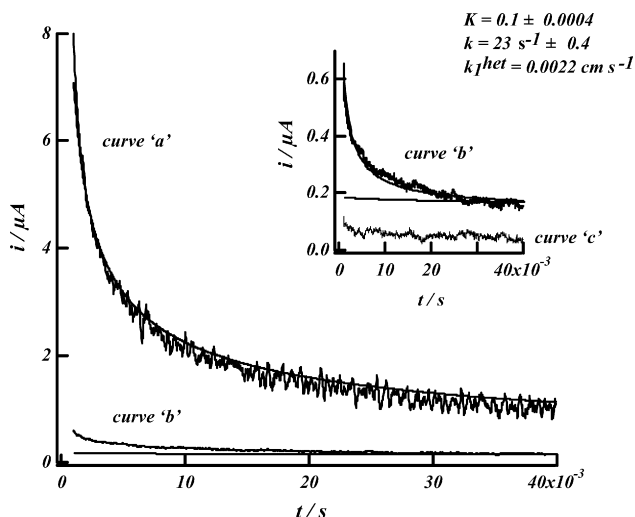


Fig. 6. Current transients in response to potential steps applied to mercury electrodes in 0.1 mol dm^{-3} KCl and $0.001 \text{ mol dm}^{-3}$ phosphate buffer with $10^{-4} \text{ mol dm}^{-3}$ Tl. Curve 'a': transient arising from potential step (-0.2 to -0.7 V) applied to uncoated mercury with no peptide in solution. Comparison transient calculated from Cottrell equation (solid line). Curves 'b' and 'c': transients arising from potential step -0.2 to -0.7 V at DOPC coated electrode with $2.24 \mu\text{mol dm}^{-3}$ peptides, P11-7 (curve 'b'), and P13-1 (curve 'c') in solution, respectively. Fit of the exact (solid line) Eq. (2) describing the current transient resulting from a C_rE_r electrode mechanism following a potential step. K and k fitting errors expressed as \pm S.D. Current transient calculated from approximate C_rE_r Eq. (3) using extracted coefficients K and k (solid line).

wave with peptide concentration in solution. The remaining peptides facilitate TI^+ reduction to a lesser extent. The form of TI^+ reduction across the P11-2 and P11-7 modified DOPC layer shows some form of plateau current whereas TI^+ reduction through the P11-1 modified DOPC monolayer increases irregularly with increase in applied negative potential.

Fig. 6 shows the nature of the TI^+ reduction current transient following a voltage pulse from -0.2 to -0.6 V applied to the P11-7 modified DOPC coated electrode. The current transient of TI^+ reduction at an uncoated mercury surface is shown for comparison. The current transient at the uncoated mercury surface conforms as expected to the Cottrell equation. The current transient at the peptide modified DOPC coated electrode fits Eq. (2) and thus emulates that observed for a C_rE_r reduction. At longer time scales the current transient assumes the characteristics of that expected for the diffusion of an ion to a heterogeneous reaction and the plot for this is generated and displayed using the coefficients K and k extracted from the fit of Eq. (2) to the data. The initial decay in the transient fitted to Eq. (2) could be interpreted as a relaxation of time constant $\sim k^{-1}$ due to a conformational change in the peptide. Values of K and k and k_1^{het} which are a measure of TI^+ permeability in the monolayer extracted from the Eq. (2) fit are displayed in Fig. 6.

4. Discussion

4.1. Peptide interaction with phospholipid

Peptide interaction with DOPC depresses the capacitance peaks because the peaks relate to phospholipid phase transitions whose occurrence is sensitive to the structure of the layer [33]. In addition the capacitance peaks on the anodic scan show greater depression than those on the cathodic scan. The reason for this is that the anodic scan follows a cathodic scan during which the potential is taken to a negative value, -1.2 V, where the phospholipid layer is more permeable. In this state the monolayer will be more available for interaction with the peptide than in the impermeable state during the cathodic scan.

The effect of the monolayer active peptides on the impedance data is similar to that of gramicidin A [33]. The introduction of the extra capacitive element in the complex capacitance plot is related to the introduction of inhomogeneity into the monolayer. This concurs with an increase in the ZFC which is related to a peptide of higher dielectric constant penetrating the monolayer. The result is also commensurate with the results from the application of Eq. (1) to the data which shows a significant decrease of β from unity associated with "surface roughness". Of interest is the α value which is less than that observed from gramicidin interaction with DOPC [33]. A tentative explanation could be that the gramicidin interaction leads to single molecule channels penetrating the monolayer whereas the self-assembling peptide permeabilisation is due to assemblies of peptide penetrating the layer. These assemblies in contrast to single molecular channels give rise to a more diffuse time constant in their relaxation in the ac field.

The data from the capacitance–potential curves and the impedance–frequency plots in the complex capacitance plane categorise the peptides into two groups which relate to the extent of interaction which they have with the DOPC monolayer. The first group contains the peptides which interact weakly with the monolayer namely P11-6 and P11-1 and the second group contains peptides which interact more strongly with the monolayer namely P11-2, P13-1 and P11-7. The main feature which separates these two groups is the presence/absence of the aromatic residues tryptophan and phenylalanine (see Scheme 1). Clearly the presence of such aromatic amino acid residues in the peptide promotes interaction with the DOPC.

Out of the three peptides which interact more strongly with the phospholipid monolayer, P11-2 permeabilises the layer to TI^+ to the greatest extent. Permeabilisation can be due to either disruption of the monolayer structure or channel formation. The similarity of the sampled-current voltammetry plots to those facilitated on modification of DOPC with gramicidin suggests that channel formation by the peptide might be the factor increasing permeability. The form of the current–time transient taken from the top of the current plateau is indicative also of channel control of TI^+ transport through the

monolayer and is similar to that resulting from gramicidin channel transport. Further tests would need to be done with other redox active ions to confirm channel activity from the peptide. The transient shows the relaxation interpreted previously as a conformational change associated with the peptide. This relaxation is of longer duration ($k^{-1} \sim 45$ ms) than that associated with the gramicidin channel transport of Ti^+ ($k^{-1} \sim 4$ ms). The value of k_1^{het} of $2 \times 10^{-3} \text{ cm s}^{-1}$ with $2.24 \mu\text{mol dm}^{-3}$ P11-7 in the electrolyte is smaller than the value of k_1^{het} of $\sim 9 \times 10^{-3} \text{ cm s}^{-1}$ due to gramicidin permeabilisation with only $0.013 \mu\text{mol dm}^{-3}$ gramicidin A in the electrolyte.

The increase in the ZFC resulting from peptide interaction indicates penetration of the DOPC dielectric by P11-2, P11-7 and P13-1 (which is commensurate with channel formation by the peptide) but not for P11-6 or P11-1. A rather odd finding is that P13-1 which interacts with and penetrates the phospholipid layer does not permeabilise the layer to Ti^+ . An explanation for this is that due to the increased number of residues, the secondary structure of the peptide is not able to form an ion conducting moiety in the phospholipid layer since the peptide length may not be compatible with the thickness of the layer. A further anomaly is described in the following. Peptide P11-1 does not show a significant interaction with or penetration into the DOPC layer at low solution peptide concentrations. However, this peptide facilitates the permeability of Ti^+ in the DOPC layer. The impedance data of DOPC–P11-1 interaction suggests that channel formation is unlikely thus the only explanation is that the peptide adsorbs on the layer and this affects the distribution of DOPC in the monolayer which facilitates Ti^+ permeability.

4.2. Comparison with natural antimicrobial peptides

Based on the ac voltammetry data, the self-assembling peptides appear to have a less destructive behaviour on the DOPC monolayer compared with the antimicrobial peptide magainin (2) [54,55]. Preliminary data obtained for magainin (2) at 0.03 – $0.13 \mu\text{mol dm}^{-3}$ peptide concentration (data not shown) display the same effect as that which the most DOPC-active self-assembling peptides display at $2.24 \mu\text{mol dm}^{-3}$ peptide concentration. Ti^+ permeability data supported these data. In particular the addition of $0.06 \mu\text{mol dm}^{-3}$ of antimicrobial peptide magainin (2) in solution facilitated Ti^+ permeability through the monolayer five times more efficiently than the addition of $2.24 \mu\text{mol dm}^{-3}$ of P11-2. Gramicidin A also renders monolayers of DOPC four times more permeable to Ti^+ at concentrations of gramicidin in solution 100 times lower than the self-assembling peptide (see above).

The self-assembling peptides also appear to have a less destructive behaviour on the DOPC monolayer compared with the antimicrobial peptide gramicidin A. About $0.13 \mu\text{mol dm}^{-3}$ of gramicidin A peptide in solution depresses the DOPC capacitance peak (capacitance peak 1, cathodic scan) to $\sim 25 \mu\text{F cm}^{-2}$ [33]. A similar capacitance peak depression is obtained only with the addition of pep-

ptide P11-2 at $1.12 \mu\text{mol dm}^{-3}$ concentration in solution (see Fig. 1). All the other peptides cause less capacitance peak depression at all concentrations. Part of the reason for the increased ability of magainin (2) and gramicidin A to partition into the monolayer at much lower solution concentration is their water insolubility and hence greater hydrophobicity than the synthetic self-assembling peptides.

4.3. Self-assembling state of the peptides in solution prior to interaction with the lipid monolayer

The insertion and self-assembly behaviours of the peptides in the lipid monolayer can only be thoroughly understood if there is also a thorough understanding of the peptide self-assembly behaviour in the electrolyte solution, i.e. the peptide state prior to interactions with the lipid monolayer.

Previous studies have investigated the self-assembling behaviour of peptides P11-1, P11-2, P11-6, P11-7 and P13-1 in a variety of solution conditions. The critical concentrations (c^*) of peptide in solution necessary for the start of β -sheet self-assembly has thus been identified: $7 \pm 1 \mu\text{mol dm}^{-3}$ for P11-1 [42], $45 \pm 15 \mu\text{mol dm}^{-3}$ for P11-2 [37], $8 \pm 2 \mu\text{mol dm}^{-3}$ for P11-6 [42], $80 \pm 20 \mu\text{mol dm}^{-3}$ for P11-7 [43] and $<2 \mu\text{mol dm}^{-3}$ for P13-1 [42]. These self-assembling studies in solution have been carried out at neutral $\text{pH} \sim 7$ in water in the absence of salt (low ionic strength solutions). The electrochemical cell used for the studies presented here was filled with aqueous solution at neutral $\text{pH} \sim 7.6$ in the presence of 0.1 mol dm^{-3} KCl and $0.001 \text{ mol dm}^{-3}$ phosphate buffer. c^* values for zwitterionic peptides are not expected to be significantly affected by the ionic strength of the solution. Therefore, we may assume that the c^* values determined for low ionic strength solution may also apply for the peptides in the aqueous solution in the electrochemical cell. If this assumption is correct then all the electrochemical studies of peptides P11-1, P11-2, P11-6 and P11-7 carried out with peptide concentration $4.45 \text{ mmol dm}^{-3}$ ($<c^*$) or less, involved predominantly interactions of monomeric peptides from solution with the lipid monolayer rather than interactions of self-assembled β -sheet peptide tapes with the lipid monolayer. However, the situation is exactly the opposite one for P13-1, due to its very low c^* compared to all the other peptides. All the electrochemical experiments carried out with P13-1 employed peptide solutions with peptide concentrations higher than c^* . Therefore, in all the electrochemical studies presented here, P13-1 is expected to interact with the lipid monolayer as a mixture of monomeric peptides in coexistence with self-assembled β -sheet tapes and fibrils.

4.4. Peptide interactions with a phospholipid monolayer versus peptide interactions with a phospholipid bilayer

The interaction and self-assembly behaviour of peptides P11-2, P11-7 and P13-1 with a black lipid membrane (BLM technique) consisting of phosphatidylethanolamine (PE) and PC have been previously studied [44]. All three peptides

were found to penetrate the lipid bilayer and to self-assemble into discrete transmembrane pores that acted as ion-channels. P11-2 formed well-defined ion channels with low conductance values. P11-7 formed ion selective channels with a similar conductance as P11-2 as well as occasional channels with higher conductance.

P13-1 proved to be the most bilayer active of all three peptides. Compared with the other two peptides, it formed a far greater number of transmembrane channels. Furthermore P13-1 channels had heterogeneous conductance values reaching in certain cases very high values, indicating formation of very large transmembrane pores. P13-1 has a higher overall fraction of hydrophobic character than P11-2 and P11-7. Therefore, P13-1 is expected to be characterised by a higher lipid membrane–water partition coefficient than P11-2 and P11-7 and thus to have a higher tendency to partition into the phospholipid membrane. In addition the longer hydrophobic side of P13-1 is thought to match the hydrophobic thickness of the lipid bilayer better, therefore P13-1 transmembrane channels are expected to be more stable than those of P11-2 and P11-7.

Attenuated total reflection infrared spectroscopy (ATR-IR) of P13-1 in PC lipid membranes indicated the formation of transmembrane porin-like β -barrel pores [44]. These BLM and ATR-IR results of peptide interactions with a lipid bilayer are partly consistent with the results of the present study which reveal lipid interaction and facilitation of Ti^+ permeability caused by P11-2 and P11-7. However, the behaviour of P13-1 is different when in contact with the lipid bilayer as opposed to the lipid monolayer. The data of the present study reveal a significant interaction of P13-1 with the lipid monolayer but no increased Ti^+ permeability. This may be due to a different arrangement of P13-1 in the lipid monolayer compared to the bilayer, due to their different hydrophobic thicknesses.

5. Conclusions

The results show that the phospholipid-coated mercury electrode can be used as an effective screening system for the phospholipid membrane-activity of synthetic peptides, including self-assembling peptides. This conclusion is based on the following findings:

1. Out of five systematically varied β -sheet self-assembling peptides tested in the present study, P11-2, P11-7 and P13-1 amphiphilic peptides, containing a tryptophan residue each, showed the strongest interaction with a monolayer of DOPC. This was based on impedance data of the DOPC coated electrode. The same peptides in concurrent studies have been shown to penetrate and modify phospholipid bilayers.
2. The P11-2 and P11-7 amphiphilic peptides containing tryptophan facilitated some permeability to Ti^+ on interaction with DOPC. The P11-1 polar peptide not containing a tryptophan residue, surprisingly, also facilitated permeability to Ti^+ .
3. All self-assembling peptides were found to interact with DOPC in a much weaker manner compared to the natural antimicrobial peptides magainin (2) and gramicidin A.

Acknowledgements

Funding for this work was provided by the Joint Grant Scheme (MoD-NERC) and the EPSRC Grant Ref. GR/R67439. A. Aggeli gratefully acknowledges the financial support of the Royal Society through a personal Royal Society University Research Fellowship.

References

- [1] La Rocca P, Biggin PC, Tieleman DP, Sansom MS. Simulation studies of the interaction of antimicrobial peptides and lipid bilayers. *Biochim Biophys Acta* 1999;1462:185–200.
- [2] Maget-Dana R. The monolayer technique: a potent tool for studying the interfacial properties of antimicrobial and membrane-lytic peptides and their interactions with lipid membranes. *Biochim Biophys Acta* 1999;1462:109–40.
- [3] Papo NY, Shai Y. Can we predict biological activity of antimicrobial peptides from their interactions with model phospholipid membranes? *Biochemistry* 2003;42:458–66.
- [4] Dathe M, Meyer J, Beyermann M, Maul B, Hoischen C, Bienert M. General aspects of peptide selectivity towards lipid bilayers and cell membranes studied by variation of the structural parameters of amphipathic helical model peptides. *Biochim Biophys Acta* 2002;1558:171–86.
- [5] van't Hof W, Veerman EC, Helmerhorst EJ, Amerongen AV. Antimicrobial peptides: properties and applicability. *Biol Chem* 2001;382:597–619.
- [6] Huang HW. Action of antimicrobial peptides: two-state model. *Biochemistry* 2000;39:8347–52.
- [7] Killian JA, von Heijne G. How proteins adapt to a membrane–water interface. *Trends Biochem Sci* 2000;9:429–34.
- [8] Cserhati T, Szogyi M. Interaction of phospholipids with proteins and peptides: new advances IV. *Int J Biochem* 1994;26:1–18.
- [9] van Kan EJ, Demel RA, Breukink E, van der Bent A, de Kruijff B. Clavanin permeabilizes target membranes via two distinctly different pH-dependent mechanisms. *Biochemistry* 2002;41:7529–39.
- [10] Zasloff M. Antimicrobial peptides of multicellular organisms. *Nature* 2002;415:389–95.
- [11] Shai Y. Mechanism of the binding, insertion and destabilization of phospholipid bilayer membranes by alpha-helical antimicrobial and cell non-selective membrane-lytic peptides. *Biochim Biophys Acta* 1999;1462:55–70.
- [12] Chen FY, Lee MT, Huang HW. Evidence for membrane thinning effect as the mechanism for peptide-induced pore formation. *Biophys J* 2003;84:3751–8.
- [13] Juvvadi P, Vunnam S, Merrifield RB. Hydrophobic effects on antibacterial and channel-forming properties of cecropin A-melittin hybrids. *J Am Chem Soc* 1996;118:8989–97.
- [14] Ehrenstein G, Lecar H. Electrically gated ionic channels in lipid bilayers. *Q Rev Biophys* 1977;10:1–34.
- [15] Christensen B, Fink J, Merrifield RB, Mauzerall D. Channel-forming properties of cecropins and related model compounds incorporated into planar lipid membranes. *Proc Natl Acad Sci USA* 1988;85:5072–6.
- [16] Matsuzaki K, Harada M, Handa T, Funakoshi S, Fujii N, Yajima H, et al. Magainin 1-induced leakage of entrapped calcein out of

- negatively charged lipid vesicles. *Biochim Biophys Acta* 1989;981:130–4.
- [17] He K, Ludtke SJ, Worcester DL, Huang HW. Mechanism of alamethicin insertion into lipid bilayers. *Biophys J* 1996;70:2659–66.
- [18] Pouny Y, Rapaport D, Mor A, Nicolas P, Shai Y. Interaction of antimicrobial dermaseptin and its fluorescently labeled analogues with phospholipid membranes. *Biochemistry* 1992;31:12416–23.
- [19] Wu M, Maier E, Benz R, Hancock RE. Mechanism of interaction of different classes of cationic antimicrobial peptides with planar bilayers and with the cytoplasmic membrane of *Escherichia coli*. *Biochemistry* 1999;38:7235–42.
- [20] Mor A, Nicolas P. The NH₂-terminal alpha-helical domain 1–18 of dermaseptin is responsible for antimicrobial activity. *J Biol Chem* 1994;269:1934–9.
- [21] Matsuzaki K, Murase O, Fujii N, Miyajima K. An antimicrobial peptide, magainin 2, induced rapid flip-flop of phospholipids coupled with pore formation and peptide translocation. *Biochemistry* 1996;35:11361–8.
- [22] Ludtke SJ, He K, Heller WT, Harroun TA, Yang L, Huang HW. Membrane pores induced by magainin. *Biochemistry* 1996;35:13723–8.
- [23] Anderlueh G, Dalla Serra M, Viero G, Guella G, Macek P, Menestrina G. Pore formation by equinatoxin II, a eukaryotic protein toxin, occurs by induction of nonlamellar lipid structures. *J Biol Chem* 2003;278:45216–23.
- [24] Gallucci E, Meleleo D, Micelli S, Picciarelli V. Magainin 2 channel formation in planar lipid membranes: the role of lipid polar groups and ergosterol. *Eur Biophys J* 2003;32:22–32.
- [25] Tang YC, Deber CM. Aqueous solubility and membrane interactions of hydrophobic peptides with peptoid tags. *Biopolymers* 2004;76:110–8.
- [26] de Planque MR, Boots JW, Rijkers DT, Liskamp RM, Greathouse DV, Killian JA. The effects of hydrophobic mismatch between phosphatidylcholine bilayers and transmembrane alpha-helical peptides depend on the nature of interfacially exposed aromatic and charged residues. *Biochemistry* 2002;41:8396–404.
- [27] Salay LC, Procopio J, Oliveira E, Nakaie CR, Schreier S. Ion channel-like activity of the antimicrobial peptide tritriptin in planar lipid bilayers. *FEBS Lett* 2004;565:171–5.
- [28] Maltseva E, Brezesinski G. Adsorption of amyloid beta (1–40) peptide to phosphatidylethanolamine monolayers. *Chemphyschem* 2004;5:1185–90.
- [29] Kim JM, Patwardhan A, Bott A, Thompson DH. Preparation and electrochemical behavior of gramicidin-bipolar lipid monolayer membranes supported on gold electrodes. *Biochim Biophys Acta* 2003;1617:10–21.
- [30] Bizzotto D, Nelson A. Continuing electrochemical studies of phospholipid monolayers of dioleoyl phosphatidylcholine at the mercury–electrolyte interface. *Langmuir* 1998;14:6269–73.
- [31] Nelson A. Conducting gramicidin channel activity in phospholipid monolayers. *Biophys J* 2001;80:2694–703.
- [32] Whitehouse C, O’Flanagan R, Lindholm-Sethson B, Movaghar B, Nelson A. Application of electrochemical impedance spectroscopy to the study of dioleoyl phosphatidylcholine monolayers on mercury. *Langmuir* 2004;20:136–44.
- [33] Whitehouse C, Gidalevitz D, Cahuzac M, Koeppe II RE, Nelson A. Interaction of gramicidin derivatives with phospholipid monolayers. *Langmuir* 2004;20:9291–8.
- [34] Aggeli A, Bell M, Boden N, Keen J, Knowles PF, McLeish TCB, et al. Responsive gels formed by the spontaneous self-assembly of peptides into polymeric, β -sheet tapes. *Nature* 1997;386:259–62.
- [35] Aggeli A, Bell M, Boden N, Keen JN, McLeish TCB, Nyrkova I, et al. Engineering of peptide-based β -sheet nanotapes. *J Mater Chem Special Issue: Mol Assemblies Nanochem* 1997;7:1135–45.
- [36] Aggeli A, Boden N, Fytas G, McLeish TCB, Mawer P, Vlassopoulos D. Structure and dynamics of self assembled peptide polymeric β -sheet tapes by dynamic light scattering. *Biomacromolecules* 2001;2:378–88.
- [37] Aggeli A, Nyrkova I, Bell M, Harding R, Carrick L, McLeish TCB, et al. Hierarchical self-assembly of chiral units as a model for β -sheet macromolecules which form gels and liquid crystals. *Proc Natl Acad Sci USA* 2001;98:11857–62.
- [38] Nyrkova IA, Semenov AN, Aggeli A, Boden N. Fibril stability in solutions of twisted β -sheet peptides: a new kind of micellisation in chiral systems. *Eur Phys J B* 2000;17:481–97.
- [39] Nyrkova IA, Semenov AN, Aggeli A, Boden N. Fibril stability in solutions of twisted β -sheet peptides: a new kind of micellisation in chiral systems. *Eur Phys J B* 2000;17:481–97.
- [40] Aggeli A, Bell M, Carrick L, Fishwick C, Harding R, Mawer P, et al. pH as a trigger of peptide β -sheet self-assembly and reversible switching between nematic and isotropic phases. *JACS* 2003;125:9619–28.
- [41] Aggeli A, Bell M, Boden N, Carrick L, Strong A. Self-assembling peptide polyelectrolyte β -sheet complexes form nematic hydrogels. *Angewandte Chim* 2003;42:5603–6.
- [42] Carrick LM. PhD Thesis. SOMS, School of Chemistry, University of Leeds; 2002.
- [43] Kioupritzi E. Masters Thesis. SOMS, School of Chemistry, University of Leeds; 2003.
- [44] Salay LC. PhD Thesis. SOMS, School of Chemistry, University of Leeds; 2002.
- [45] Wiegand G, Arribas-Layton N, Hillebrandt H, Sackmann E, Wagner P. Electrical properties of supported lipid bilayer membranes. *J Phys Chem B* 2002;106:4245–54.
- [46] Janek RP, Fawcett WR, Ulman AJ. Impedance spectroscopy of self-assembled monolayers on Au(111): evidence for complex double-layer structure in aqueous NaClO₄ at the potential of zero charge. *Phys Chem B* 1997;101:8550–8.
- [47] Lindholm-Sethson B. Electrochemistry at ultrathin organic films at planar gold electrodes. *Langmuir* 1996;12:3305–14.
- [48] Strašák L, Dvořák J, Hason S, Vetterl V. Electrochemical impedance spectroscopy of polynucleotide adsorption. *Bioelectrochemistry* 2002;56:37–41.
- [49] Peng Diao P, Jiang D, Cui X, Gu D, Tong R, Zhong B. Studies of structural disorder of self-assembled thiol monolayers on gold by cyclic voltammetry and ac impedance. *J Electroanal Chem* 1999;464:61–7.
- [50] Lingler S, Rubinstein I, Knoll W, Offenhausser A. Fusion of small unilamellar lipid vesicles to alkanethiol and thiolipid self-assembled monolayers on gold. *Langmuir* 1997;13:7085–91.
- [51] Macdonald DD. *Transient techniques in electrochemistry*. New York: Plenum Press; 1977. p. 96–100.
- [52] Nelson A, Bizzotto D. Chronoamperometric study of Tl(I) reduction at gramicidin-modified phospholipid-coated mercury electrodes. *Langmuir* 1999;15:7031–9.
- [53] Galus Z. *Fundamentals of electrochemical analysis*. 1st ed. Chichester, UK: Ellis Horwood; 1977. p. 335–86.
- [54] Wakamatsu K, Takeda A, Tachi T, Matsuzaki K. Dimer structure of magainin 2 bound to phospholipid vesicles. *Biopolymers* 2002;64:314–27.
- [55] Mukai Y, Matsushita Y, Niidome T, Hatekeyama T, Aoyag HJ. Parallel and antiparallel dimers of magainin 2: their interaction with phospholipid membrane and antibacterial activity. *Pept Sci* 2002;8:570–7.